Research Article

Journal of Physical Organic Chemistry

Received: 30 June 2013, Revised: 15 August 2013, Accepted: 10 October 2013, Published online in Wiley Online Library: 12 November 2013

(wileyonlinelibrary.com) DOI: 10.1002/poc.3250

Non-covalent interactions in receptor–ligand complexes. A study based on the electron charge density

Emilio L. Angelina[a,c]*, Sebastián A. Andujar[b,c], Rodrigo D. Tosso[b,c], Ricardo D. Enriz[b,c] and Nélida M. Peruchena[a]*

In this paper, we reported the results obtained by charge density analysis of the network of non-covalent interactions (NCI) established in the binding pocket of a receptor, in relevant conformations of ligand – receptor complexes. Starting with strong and moderate hydrogen bonds, moving on to weaker polar interactions and ending with stacking and T-shape like interactions between aromatic rings, all of them have been investigated within the framework of the density functional theory and the quantum theory of atoms in molecules. Also, natural bond orbital analysis was carried out, in order to evaluate quantitatively the electronic population of the aromatic rings. The analysis of our "case study" shows that the interactions of the catechol OH groups of the ligand, in the different conformations of the dopamine (DA) – D2 receptor complex, determine the decrease or increase of the electron density on the aromatic ring of DA. In turn, the electronic population of the aromatic ring of DA defines its orientation within the binding site and the type of interactions that it establishes with the aromatic rings of the receptor. Although the approach used here was traditionally applied to the study of NCI in small molecules complexes in gas phase, we show through this work that this methodology is also a very powerful tool for the study of biomolecular complexes, providing a very detailed description of the binding event. Copyright © 2013 John Wiley & Sons, Ltd.

Keywords: DFT; D2–dopamine receptor; NBO; QTAIM; stacking interaction

INTRODUCTION

One of the most motivating facts for studying the non-covalent interactions (NCI) is that they are responsible for the structure and dynamics and, consequently, also the function of biological macromolecules.[1] Thus, for example, the interaction of a hormone with a receptor can produce a cascade of processes many of them closely related to the formation or rupture of NCI.[2] Consequently, the understanding of NCI in biomolecular complexes constitutes a bulky challenge.

The term "non-covalent" seems to be reserved for intra- and intermolecular interactions which are not classified as typical covalent bonds, but they are important for the stabilization of biomolecular systems.[3,4] Hydrogen bonds are by far the most important specific interactions in biological recognition processes. However, other interactions ranging from strongly electrostatic to strongly dispersive such as, for example, the dihydrogen bonds, halogen bonds, stacking interactions, dispersion interactions, and X–H···π interactions have been the subject of extensive investigations.[5,6] Several of these interactions have been extensively studied in our laboratory.[7–9] As the NCI generally are weaker than covalent interactions, they are more difficult to describe properly. However, recent advances in computational calculation of the electron charge density make possible the proper description of the three-dimensional network of bonding and non bonding interactions (molecular graphs) in biological systems in the context of the quantum theory of atoms in molecules (QTAIM).[5,10,11] Starting with strong and moderate hydrogen bonds or halogen bonds, moving on to weaker polar interactions and ending with stacking and T-shape interactions between aromatic rings, all them can be evaluated by QTAIM.[3] In fact, nowadays it is well know that the stacking of aromatic amino acids in proteins is evidently much more important than it has been previously believed and, indeed, can form one of the dominant stabilizing contributions.[10]

In complex biological systems, the NCI (i.e. H-bonds) may operate simultaneously, giving rise to interesting cooperative effects among them. As is well-known, when they occur simultaneously, the collective strength of the set of H-bonds is larger than the sum of the strength of the individual bonds.[12–16] However, in computational medicinal chemistry, the molecular

* *Correspondence to: Emilio L. Angelina and Nélida M. Peruchena, Lab. Estructura Molecular y Propiedades, Área de Química Física, Departamento de Química, Facultad de Ciencias Exactas y Naturales y Agrimensura, Universidad Nacional del Nordeste. Av. Libertad 5470, Corrientes (3400), Argentina. E-mail: emilioluisangelina@gmail.com; arabeshai@yahoo.com.ar*

a *E. L. Angelina, N. M. Peruchena*
Lab. Estructura Molecular y Propiedades, Área de Química Física, Departamento de Química, Facultad de Ciencias Exactas y Naturales y Agrimensura, Universidad Nacional del Nordeste, Av. Libertad 5470, Corrientes 3400, Argentina

b *S. A. Andujar, R. D. Tosso, R. D. Enriz*
Departamento de Química, Facultad de Química, Bioquímica y Farmacia, Universidad Nacional de San Luis, Chacabuco 917, San Luis (5700), San Luis, Argentina

c *E. L. Angelina, S. A. Andujar, R. D. Tosso, R. D. Enriz*
Instituto Multidiciplinario de Investigaciones Biológicas (IMIBIO-SL, CONICET), Chacabuco y Pedrenera (5700) San Luis, Argentina

recognition process is usually described with non quantum mechanical methods based on the concept of pair-wise interactions, wherein the contributions of such pairs are treated independently and additively, when actually all interactions are influenced by neighboring groups. In fact, in our case study about dopamine (DA) into the D2 DA receptor (D2R) (see below), the catechol hydroxyl groups from the DA molecule might act simultaneously as proton donors (H-donors) and as proton acceptors (H-acceptors); therefore, a molecular mechanic treatment of these interactions would underestimate the strength of the H-bonds.

Moreover, it has been recently shown that the Classical Molecular Dynamic simulation of different ligands in the binding site of the receptor discriminates well between very strong and poor binders but it is not accurate enough to distinguish between binders in the intermediate range of anchoring strength. However, when the system is reduced to a 3D model containing only the relevant residues from the binding pocket, it can be treated quantum mechanically and the correlation with the experimental binding affinities is quite better for the entire range of binding strengths.[17,18] Besides the observed energetic improvement, the reduced model (RM) also enables one to compute the charge density molecular graphs of the binding site. Among the electron density parameters, the electron density evaluated at the interaction bond critical point (ρ_b) has proven to be a good estimation of the strength of the linkage.[19–21] Furthermore, in a recent study about microhydration of cycloether molecules, a linear relationship was found between the solute–solvent interaction energy and the sum of the ρ_b values between the cycloether and each one of the water molecules ($\Sigma\rho_b$).[22] Thus, through the charge density treatment of the RM, it is possible to decompose the total interaction energy into contributions from the different groups of the ligand molecule and to provide an estimation of the anchoring strength of each group into the binding pocket. This strategy was applied recently to evaluate the interactions of a set of compounds that bind to the catalytic site of the human dihydrofolate reductase.[18]

As a case study, in this work, we evaluate the NCI of DA in the D2R. Several important diseases of the nervous system are associated with dysfunctions of the DA system. Parkinson's disease is caused by loss of DA-secreting neurons in the midbrain area called the substantia nigra. There is evidence that schizophrenia involves altered levels of DA activity, and the antipsychotic drugs that are frequently used to treat it have a primary effect of attenuating DA activity.[23,24] Due to the presence of the N-cation in solution at physiological pH[25] and based on previous results obtained in different conditions (in vacuo and in solution, making use of small models as well as DA itself or other catecholamines), DA was simulated protonated.[25] In addition, previous theoretical calculations reported by Andujar *et al*.[26] suggested that a mechanistic stepwise process takes place for DA in which the protonated nitrogen group (in any conformation) acts as the anchoring portion, and this process is followed by a rapid rearrangement of the conformation, allowing the interaction of the catecholic OH groups. A theoretical study performed by Nishihira and Tachnikawa[27] reported that the protonated form became energetically more stable than the neutral molecule by 12.00 eV. This indicated that DA was stable as a cationic molecule. Such results suggested that DA bound to the receptor as a cationic molecule protonated at the side chain amino group. In addition Borštnar *et al*.[28] reported potentially favorable cation–π interactions between the $-NH_3^+$ group on DA and aromatic moieties, which provide a stabilizing effect to the charged fragment. Thus, we offer here theoretical evidence that the amine is most likely to be present in the active site in its protonated form, which is similar to the conclusion from experimental studies of monoamine oxidase A.[29]

Taking advantage of structural information available from previous experimental and theoretical studies of DA–D2R complexes,[26] we performed a study of DA interacting with D2R by using a RM of several selected conformations of the DA–D2R complex (with only 13 amino acids of the binding pocket of the receptor) that were used as input for the calculation of the charge density molecular graphs. These conformations were previously obtained from an exhaustive and complete conformational study on the potential energy hypersurface of DA interacting with D2R.[26] The common characteristic displayed for all of the complexes is a strong interaction between the protonated amino group of DA and Asp86. On the basis of the different spatial orderings adopted by DA and its receptor, as well as the different intermolecular interactions observed, the 46 conformations obtained were clusterized in five different types (A–E). The results allow the authors to postulate the complexes of type A as the "biologically relevant conformations" of DA. The common feature of the type A complexes is that they adopt an adequate conformation to allow interactions between the OH groups of the catechol ring with a cluster of serines formed by Ser141, Ser144, and Ser118. Mutagenesis of the cloned DA and related monoaminergic receptors combined with drug binding experiments have spotlighted that Asp86 and the group of serines are one of the most important residues for primary signal binding.[30] However, in the D2R binding pocket, there are also several aromatic residues whose relevance in the molecular recognition process remains unknown. While each individual interaction between these aromatic residues and DA might be very weak, collectively, they can make a non negligible contribution to the structure and stability of the different DA–D2R complexes.[31] Thus, one of the main goals of this work is to determine the influence of these weak aromatic interactions in the several binding modes that DA can adopt within the receptor binding pocket.

But beyond our case study, the take-home message from this work is that this kind of approach that involves the characterization of the intermolecular interactions by means of the QTAIM methodology, which traditionally has belonged to the theoretical chemists, should be also adopted by the medicinal chemists since it has proven to be a very powerful tool for the study of biomolecular complexes providing a very detailed description of the binding event.

COMPUTATIONAL DETAILS

Taking advantage of the structural information available from quantum mechanical studies of DA at the D2R, (see reference 26), we performed the charge density analysis on several selected conformations of the DA–D2R molecular complex obtained previously from our "reduced model system", with only 13 amino acids from the receptor binding pocket. The amino acids included in the RM were Phe82, Val83, Asp86, Val87, Trp115, Ser118, Ser141, Ile142, Ser144, Phe145, Trp182, Phe185, and Phe186.[26] The complexity of the system under study restricts the choice of the quantum mechanical method to be used. Therefore, single

Table 1. Calculated properties in the selected DA–D2R complexes. Number of π electrons (n_π) and change in the charge (ΔQ) of the DA ring are in *e*. Relative binding energy (ΔE) in kcal/mol

Complex[a]	ΔQ[b]	n_π[c]	ΔE[d]
1	0.021	6.1522	0.00
2	0.009	6.1783	1.54
3	−0.043	6.2082	4.18
4	−0.044	6.2093	4.53
5	−0.027	6.2118	4.78
6	0.020	6.1787	5.26

[a]Corresponding to DA–RD2*i* (*i* = 1–6) complexes denoted as 1, 2, 7, 9, 10, and 13, respectively, in reference 26.
[b]ΔQ = Q complex-Q isolated; Q was computed as the sum of the NBO charges of the DA ring carbon atoms. Positive/negative values of ΔQ are indicative of decrease/increase of electron density over the ring.
[c]n_π was computed as the sum of the electrons in π/π* bond/anti-bond orbitals.
[d]from ref 26.

point calculations were performed with the Gaussian 03 program package employing the B3LYP hybrid functional and 6-31 + G(d) as a basis set.[32] This type of calculation has been used in recent works on the topology of the charge density (ρ(r)) because it ensures a reasonable compromise between the wave function quality required to obtain reliable values of the derivatives of ρ(r) and the computer power available, due to the extension of the system in study.[5] The determination of all of the critical points of the electron charge density distribution, bond paths, local topological properties of the charge density at the critical point, as well as the display of the molecular graphs were performed with the AIMAll program.[33] Also, the natural bond orbital analysis (NBO) was performed with the NBO 3.1 program as implemented in Gaussian 03.[34]

RESULTS AND DISCUSSION

In our case study, about DA interacting with the D2R, we have chosen six of the most stable complexes from reference 26; such complexes are a representative sample of the overall series of complexes reported there. These complexes are numbered in Table 1 from the most stable to the least stable one, (*i* = 1–6). These six complexes belong to the "type A" complexes in which the catechol hydroxyl groups from the DA molecule interact with Ser118, Ser141, and/or Ser144 residues from the receptor binding site.[26]

Figure 1 shows the charge density molecular graph of DA in the binding site of D2R in complex **1** and Fig. 2 shows the molecular graphs of complexes **2, 3**, and **5**. Complexes **4** and **6** are not shown since their molecular graphs are very similar to the ones of complexes **3** and **2**, respectively.

In the molecular graphs from Figs. 1 and 2, one can see the interaction network, composed of bond critical points and bond paths that anchor the DA molecule in the binding site of the receptor. Some of these interactions, which involve the ethyl ammonium moiety of the DA molecule, are quite conserved in all the complexes studied here. The strongest of these conserved interactions is the salt bridge that involves the Asp86 carboxylate

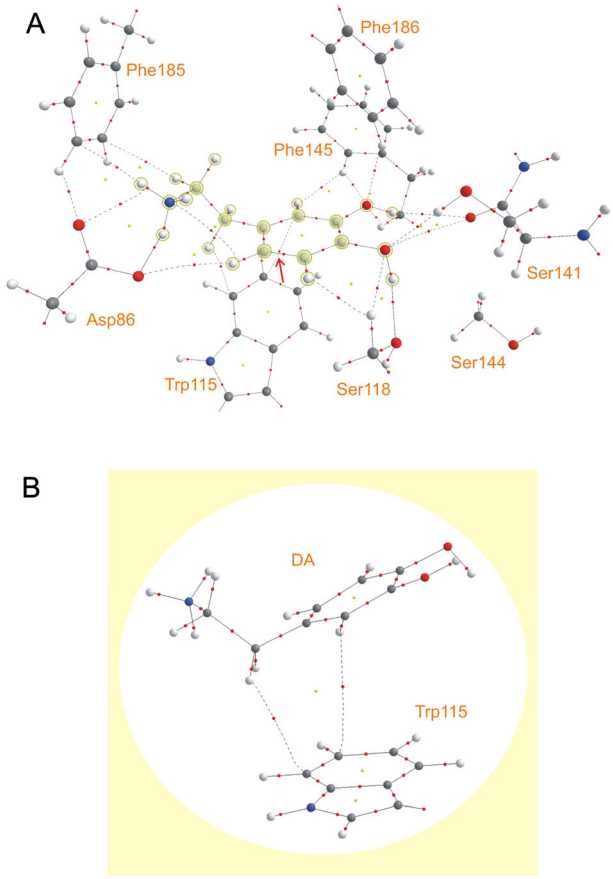

Figure 1. Charge density molecular graphs of complex **1** (A). An improved view of the DA ring stacked over the Trp115 aromatic ring is also shown (B). Big spheres correspond to attractors or nuclear critical points (3, −3), attributed to nuclei. Lines connecting the nuclei are the bond paths, and the small red spheres on them are the bond critical points or (3, −1) critical points. The small yellow spheres are ring critical points or (3,+1) critical points. The highlighted atoms correspond to the dopamine molecule, and the arrows point interactions between DA ring and the receptor aromatic rings. Some topological elements have been removed for clarity

group. This interaction is manifested in the molecular graphs by the critical points and the corresponding bond paths that connect the ammonium hydrogen atoms with the Asp86 carboxylate oxygen atoms. Also, other conserved interactions of the type C–H···π and/or N^+–H···π can be observed between the ethyl ammonium moiety from the DA molecule and the π electronic cloud from Phe185.

There are other less conserved interactions that also contribute to anchor the ethyl ammonium moiety to the binding pocket in each particular complex. For example, in complexes **1**, **2**, and **6**, two methylenic hydrogen atoms from the ethyl ammonium side chain are hydrogen bonded to aromatic carbons from Trp115 and Trp182 rings (this last residue is not shown in the molecular graphs) whereas in complexes **3**, **4**, and **5** one of these hydrogen atoms is H-bonded to a carboxylate oxygen atom from Asp86.

Moving on to the DA *para*-OH and *meta*-OH groups (from now on *p*-OH and *m*-OH, respectively), it can be seen in Figs. 1 and 2 that both *p*-OH and *m*-OH groups are acting simultaneously as H-donors and H-acceptors in the four complexes shown. As is

Journal of Physical Organic Chemistry

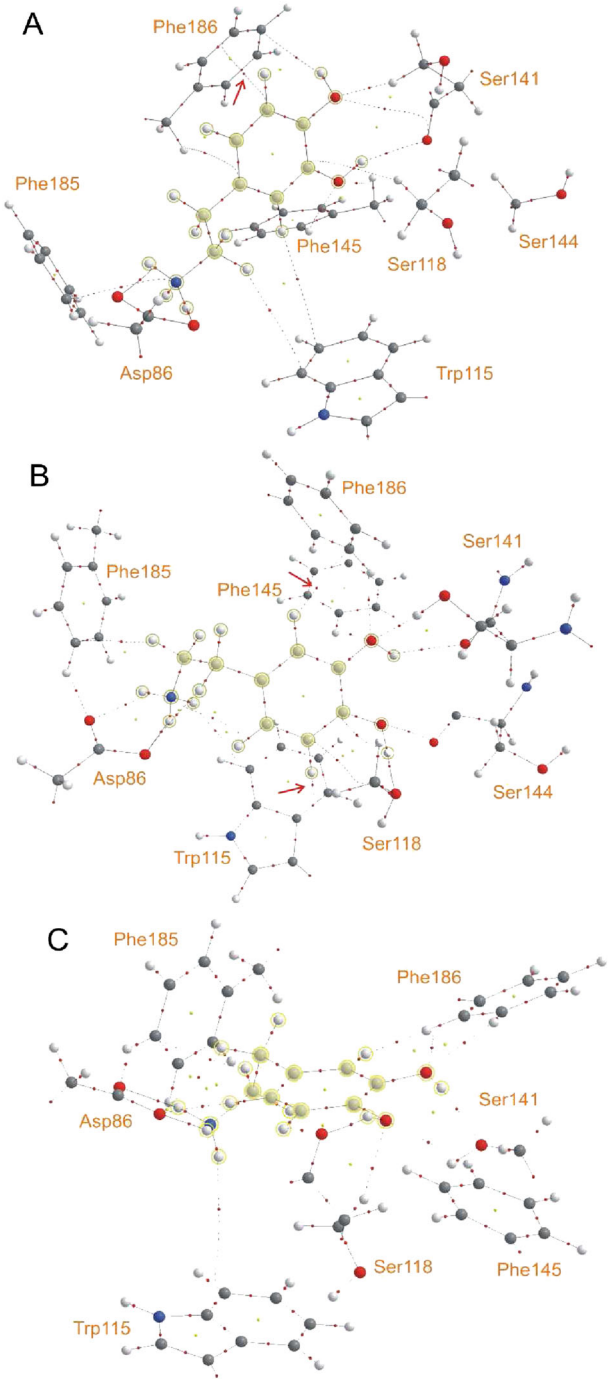

Figure 2. Charge density molecular graphs of complexes **2** (A), **3** (B), and **5** (C). Big spheres correspond to attractors or nuclear critical points (3, −3), attributed to nuclei. Lines connecting the nuclei are the bond paths, and the small red spheres on them are the bond critical points or (3, −1) critical points. The small yellow spheres are ring critical points or (3,+1) critical points. The highlighted atoms correspond to the dopamine molecule, and the arrows point interactions between DA ring and the receptor aromatic rings. Some topological elements have been removed for clarity

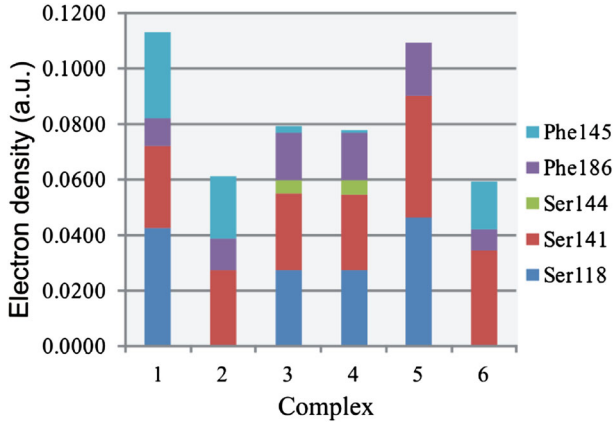

Figure 3. Sum of the electron density values ($\Sigma\rho_b$) corresponding to the interactions of the catechol hydroxyl groups which reside from the binding site, in the DA–D2R*i* (*i* = 1–6) complexes studied here

well-known, when H-bonds occur simultaneously, the collective strength of the set of H-bonds is larger than the sum of the individual bonds strength. Hence, a pair-wise treatment of these interactions as the ones employed in the molecular dynamics or docking techniques would underestimate the strength of the interactions.

Figure 3 shows the charge density values (ρ_b) at the bond critical points of the *m*-OH and *p*-OH groups interacting with residues from the receptor binding site. The total height of the stacked bars represents the strength that both catechol hydroxyl groups are anchored in the receptor binding site whereas each category indicates the contribution of a particular residue to the anchoring.

As might be seen by the total charge density values, the catechol hydroxyl groups are more strongly anchored to the receptor binding site in complex **1** which is the most stable complex, followed by complex **2**. The residues that contribute most to the anchoring are Ser118 and Ser141, but Phe145 and/or Phe186 also make important contributions.

A more detailed description of the *p*-OH and *m*-OH interaction patterns (see Fig. 1) shows that in complex **1** the *meta* hydrogen atom (*m*-H) is H-bonded to the carbonyl oxygen from Ser141 ($\rho_b = 0.0058$ au) and the *meta* oxygen atom (*m*-O) is H-bonded to two C–H bonds from Phe145 ($\rho_b = 0.0184$) and Phe186 ($\rho_b = 0.0099$) benzene rings and also to a C–H bond from the backbone of Phe145 ($\rho_b = 0.0127$). Whereas *p*-H is H-bonded to the hydroxyl oxygen atom from Ser118 ($\rho_b = 0.0288$ au) and *p*-O is H-bonded to O–H and C–H bonds from Ser141 ($\rho_b = 0.0201$ au) and Ser118 ($\rho_b = 0.0137$ au), respectively. There are also a critical point and the corresponding bond paths that connect *p*-O with the carbonyl oxygen atom from Ser141 ($\rho_b = 0.0039$ au). On the other hand, in complex **2** (and also in complex **6**), the *m*-OH group shows a similar interaction pattern than complex **1**, but the *p*-OH group interacts with the receptor binding site in a different manner. As can be seen in Fig. 2A, in complex **2** (and **6**), the *p*-H atom is interacting with the π electronic cloud of Phe186 instead of the hydroxyl oxygen atom of Ser118, as in complex **1**. In complex **3** (and also in complex **4**), both *p*-OH and *m*-OH interact in a similar fashion than in complex **1**, with the difference that in the first complexes, the Ser141 hydroxyl hydrogen atom is H-bonded to *m*-O instead of *p*-O (see Fig. 2B). Finally, in complex **5**, the *m*-H atom is H-bonded to the Ser141 hydroxyl oxygen atom rather than to Ser141 carbonyl oxygen, as in complexes **1**, **2**, and **3**, and the *p*-H atom is H-bonded to the Ser118 carbonyl oxygen rather than to Ser118 hydroxyl oxygen as in complexes **1** and **3** (see Fig. 2C).

With regard to the DA aromatic ring, it shows a different interaction pattern in the distinct complexes analyzed here. In complex **1**, the DA ring is stacked over the Trp115 indolic ring, i.e. both rings are in a quasi co-planar orientation. In consequence, a bond critical point (indicated with an arrow in the molecular graph) and the corresponding bond paths that connect an aromatic carbon from the DA ring with an aromatic carbon from the Trp115 indolic ring are observed. Besides complex **1**, this stacking-like interaction pattern of the DA ring is also observed in complex **2** (and **6**). In these last complexes, the DA ring is almost coplanar with the Phe186 aromatic ring. Consequently, a critical point and the corresponding bond paths linking a carbon atom from Phe186 ring to a carbon atom from DA ring are observed.

On the other hand, in complex **3** (and also in complex **4**), the DA ring is quasi perpendicularly orientated to the Trp115 and Phe186 aromatic rings. Due to the T-shaped like orientation among these rings, C–H···π interactions are established between them. The molecular graph of complex **3** shows a bond critical point and the corresponding bond paths that connect a hydrogen atom from the DA ring to a carbon atom from the Trp115 indolic ring. Similarly, a bond critical point and their bond paths connect another hydrogen atom from the DA ring to an aromatic carbon from the Phe186 benzene ring. Finally, in complex **5**, the DA ring is almost coplanar with the Trp115 aromatic ring, but they are too far apart so that no interaction between them is observed (the closest C···C distance between the rings is 6.4 Å in complex **5**, almost twice that of complex **1**). Tables S1 to S4 in supporting information show additional parameters for the interactions of the catechol hydroxyl groups in complexes 1, 2, 4, and 5.

Analysis of the electronic population on the DA aromatic ring

Figure 4 shows the total electrostatic potential surface superimposed to the molecular graph of complex **1**. This surface was mapped over a surface of constant molecular electron density of 0.001 au.

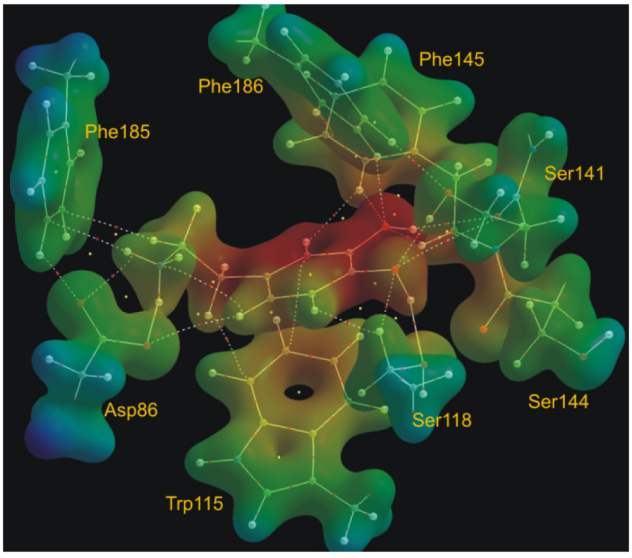

Figure 4. Molecular electrostatic potential of complex 1 mapped over a isosurface of density 0.001au. In this figure, the interaction of DA with Asp86, Trp115, Phe185,186,145, and Ser141,144,118 is shown. Also, the molecular graph is superimposed. Big circles correspond to attractors attributed to nuclei, lines connecting the nuclei are the bond paths, and the small circles on them are the BCP. The small yellow spheres correspond to ring critical points or (3,+1) critical points

The regions with the most negative values of the total electrostatic potential in this figure are the catechol oxygen atoms and the DA aromatic ring. Even when the Asp86 carboxylate and the DA ammonium groups are negatively and positively charged, respectively, they do not show extreme values of the total electrostatic potential (i.e. minimum and maximum values) due to the salt bridge formation between them that attenuates the electrostatic field generated by these charged groups.

Table 1 shows the number of π electrons of the DA ring in the DA–D2R complexes and the variation in the DA ring charge with respect to the isolated DA. The relative binding energies obtained for these complexes are also included for comparison.

The data in Table 1 show that the electronic charge of the DA aromatic ring decreases in complexes **1**, **2**, and **6** and increases in complexes **3**, **4**, and **5**, as compared with the electronic population of isolated DA. Furthermore, the number of π electrons of the aromatic ring is lower in complexes **1**, **2**, and **6** than in complexes **3**, **4**, and **5**. We have seen that in complex **1** the DA ring is stacked over the Trp115 indolic ring and in complex **2** (and in **6**) the DA ring is in a stacking-like orientation with the Phe186 benzene ring. On the other hand, in complexes **3** and **4**, the DA ring was in a T-shape-like orientation with respect to the Trp115 and Phe186 rings and in complex **5** it was too far apart from the Trp115 ring. Therefore, it seems to be a relationship between the electronic population of the DA ring and its relative orientation with respect to the aromatic rings in the binding site. The stacking-like interactions would require a low electronic population on the DA ring in order to avoid the interelectronic repulsion between the aromatic rings.

Influence of the *m*-OH and *p*-OH interaction pattern on the DA ring orientation in the receptor binding site

Since the *m*-OH and *p*-OH electronic lone pairs are delocalized over the DA aromatic ring, one might ask if the electronic population of the DA ring could be influenced by the different interaction patterns of the OH groups. Furthermore, can a deep analysis based on the electron charge density contribute to the understanding of the preferential orientation of the aromatic ring of the ligand (stacking or T-shaped) in the binding pocket?

It is expected that, as the number and strength of the H-bonds involving the *m*-O and *p*-O atoms as H-acceptors increase, the oxygen lone pairs will be less available to delocalize over the DA ring. Conversely, the greater the strength of the H-bonds involving the *m*-H and *p*-H atoms, the greater will be the availability of the oxygen lone pairs to delocalize over de DA ring, since H-bond formation leads to the polarization of the *m*-O–H and *p*-O–H H-donor bonds toward the oxygen atoms, increasing its electron donor capacity.

Table 2 shows the ratio between the ρ_b sum of all the H-bonds involving *m*-O and *p*-O as H-acceptors and the ρ_b sum of the H-bonds involving *m*-H and *p*-H as H-donors, indicated as $\sum\rho_b(m,p\text{-O})/\sum\rho_b(m,p\text{-H})$. This ratio might be considered as a measure of the availability of the catechol oxygen lone pairs to delocalize over the DA aromatic ring (the greater the ratio, the smaller the availability). Moreover, the sum of the ρ_b values at the C–O*m* and C–O*p* bond critical points, (ρ_b(C–O*m* + C–O*p*)), is also shown in Table 2. This sum might be considered as a descriptor of the delocalization degree of the lone pairs, since the delocalization of the lone pairs over the DA ring will

Journal of Physical Organic Chemistry

Table 2. Descriptors of availability[a] and delocalization degree[b] of the catechol oxygen lone pairs over the DA aromatic ring

Complex	$\Sigma\rho_b(m,p\text{-O})/\Sigma\rho_b(m,p\text{-H})$[a]	$\rho_b(\text{C–O}m + \text{C–O}p)$[b]
1	2.27	0.5565
2	1.85	0.5587
3	1.03	0.5941
4	1.00	0.5942
5	1.14	0.5947
6	1.87	0.5604

[a]dimensionless, [b]in atomic units

increase the *m*-C–O and *p*-C–O bond order and so, the ρ_b value will increase.

As can be seen in Table 2, complexes **1**, **2**, and **6** show a ratio $\Sigma\rho_b(m,p\text{-O})/\Sigma\rho_b(m,p\text{-H}) \approx 2$ whereas in complexes **3**, **4**, and **5** it takes a value close to 1. Therefore, the catechol oxygen lone pairs are less available to delocalize over the DA aromatic ring in the first complexes. Moreover, the sum $\rho_b(\text{C–O}m + \text{C–O}p)$ is smaller in complexes **1**, **2**, and **6** than in complexes **3**, **4**, and **5** suggesting a lower C–O bond order in the first complexes and hence a decreased delocalization of the catechol oxygen lone pair over the DA aromatic ring.

Note that these findings are in line with the variations found in the electronic population of the DA ring, namely the lesser the delocalization of the catechol oxygen lone pairs over the DA ring, the smaller the electronic population of that ring and vice versa.

Thus, in complexes **1**, **2**, and **6**, the decreased delocalization of the catechol oxygen lone pairs over the DA aromatic ring lowers the electronic population of the ring allowing it to be stacked over Trp115 and Phe186 rings, respectively. Conversely, in complexes **3**, **4**, and **5**, the greater delocalization of the *m*-O and *p*-O lone pairs increases the electronic population of the DA ring preventing it (via electronic repulsion) to be stacked over the aromatic rings of the receptor binding site. Therefore, the DA ring tends to be oriented perpendicularly (T-shaped) to the receptor aromatic rings as in complexes **3** and **4** or far apart from the π electronic cloud of the aromatic residues, as in complex **5**.

CONCLUSIONS

The work presented here is intended to contribute to the understanding of the NCI in the context of the ligand–receptor binding event in a two-way manner, by providing a detailed topological description of the interaction network of the ligand in the receptor binding pocket and by showing the convenience of going beyond the concept of pair-wise interactions to "see" the electronic effects within the intricate biological environment.

With regard to our case study of DA in the D2 receptor binding pocket, we have shown throughout this work that the electronic charge distribution on the DA aromatic ring undergoes significant changes due to the main interaction of the catechol hydroxyl groups with the residues from the receptor binding site. In turn, the redistribution of the electronic charge on the ligand ring determines the type of interactions it forms with the aromatic amino acid residues of the receptor in the binding pocket.

While this kind approach that involves the characterization of the intermolecular interactions by means of QTAIM was traditionally applied to the study of NCI in small molecules complexes in gas phase, we have shown through this work that this methodology is also a very powerful tool for the study of biomolecular complexes, providing a very detailed description of the binding event.

Acknowledgements

We acknowledge SECYT UNNE for financial support. E.L.A and R.D.T. are postdoctoral fellow researchers of CONICET-Argentina; S.A.A., R.D.E., and N.M.P. are career researchers of CONICET, Argentina. This work was supported by the PIP 095 CONICET.

REFERENCES

[1] P. Hobza, K. Müller-Dethlefs, Non-Covalent Interactions. Theory and Experiment, Royal Society of Chemistry Nottingham, **2010**.
[2] I. Alkorta, S. J. Grabowski, *Comput. Theor. Chem.* **2012**, *998*, 1.
[3] S. J. Grabowski, *J. Phys. Chem. A* **2012**, *116*, 1838.
[4] S. Scheiner, T. Kar, *J. Phys. Chem. B* **2005**, *109*, 3681.
[5] C. F. Matta, R. J. E. Boyd, *The Quantum Theory of Atoms in Molecules. From solid State to DNA and Drug Design*, Wiley-VCH, Weinheim, **2007**.
[6] H. M. Lee, J. Singh, K. S. Kim, in *Hydrogen Bonding - New Insights* (Ed.: S. Grabowski), Springer, Dordretch, **2006**.
[7] M. M. Vallejos, E. L. Angelina, N. M. Peruchena, *J. Phys. Chem. A* **2010**, *114*, 2855.
[8] D. J. R. Duarte, M. Vallejos, N. Peruchena, *J. Mol. Mod.* **2010**, *16*, 737.
[9] M. M. Vallejos, A. M. Lamsabhi, N. M. Peruchena, O. Mó, M. Yáñez, *J. Phys. Org. Chem.* **2012**, *25*, 1380.
[10] R. A. Mosquera, M. J. Gonzalez Moa, L. Estevez, M. Mandado, A. M. Graña, in *Quantum Biochemistry* (Ed.: C. F. Matta), WILEY-VCH Verlag GmbH & Co. KGaA, Weinheim, Germany, **2010**.
[11] R. Bader, *Atoms in Molecules: A Quantum Theory*, Oxford University Press., New York, **1990**.
[12] G. A. Jeffrey, W. Saenger, *Hydrogen bonding in Biological Structures*, Springer-Verlag, New York, **1991**.
[13] P. Gilli, V. Bertolasi, V. Ferretti, G. Gilli, *J. Am. Chem. Soc.* **1994**, *116*, 909.
[14] J. J. Dannenberg, *J. Phys. Chem. A* **2006**, *110*, 5798.
[15] N. Kobko, L. Paraskevas, E. del Rio, J. J. Dannenberg, *J. Am. Chem. Soc.* **2001**, *123*, 4348.
[16] S. Scheiner, T. Kar, *J. Phys. Chem. A* **2004**, *108*, 9161.
[17] R. D. Tosso, S. A. Andujar, L. Gutierrez, E. Angelina, R. Rodríguez, M. Nogueras, H. Baldoni, F. D. Suvire, J. Cobo, R. D. Enriz, *J. Chem. Inf. Model.* **2013**, *53*, 2018.
[18] S. Andujar, F. Suvire, I. Berenguer, N. Cabedo, P. Marín, L. Moreno, M. D. Ivorra, D. Cortes, R. D. Enriz. *J. Mol Mod.* **2012**, *18*, 419–431.
[19] R. J. Boyd, S. C. Choi, *Chem. Phys. Lett.* **1985**, *120*, 80.
[20] R. J. Boyd, S. C. Choi, *Chem. Phys. Lett.* **1986**, *129*, 62.
[21] O. Mó, M. Yáñez, J. E. Del Bene, I. Alkorta, J. Elguero, *Chem. Phys. Chem.* **2005**, *6*, 1411.
[22] M. M. Vallejos, N. M. Peruchena, *J. Phys. Chem. A* **2012**, *116*, 4199.
[23] L. L. Brunton, J. S. Lazo, K. L. Parker, *Goodman & Gilman's The Pharmacological Basis of Therapeutics*, 11th ed., McGraw-Hill, New York, **2005**.
[24] W. Schultz, *Ann. Rev. Neur.* **2007**, *30*, 259.
[25] G. Alargona, C. Ghio, *Chem. Phys.* **1996**, *204*, 239.
[26] S. A. Andujar, R. D. Tosso, F. D. Suvire, E. L. Angelina, N. M. Peruchena, N. Cabedo, D. Cortes, R. D. Enriz, *J. Chem. Inf. Mod.* **2011**, *52*, 99.
[27] J. Nishihira, H. Tachikawa, *J. Theor. Biol.* **1997**, *185*, 157.
[28] a)R. Vianello, M. Repič, J. Mavri, *Eur. J. Org. Chem*, **2012**, 7057; b)R. Borštnar, M. Repič, S. C. L. Kamerlin, R. Vianello, J. Mavri, *J. Chem. Theor. Comput.* **2012**, *8*, 3864.
[29] T. Z. E. Jones, D. Balsa, M. Unzeta, R. R. Ramsay, *J. Neur. Transm.* **2007**, *114*, 707.
[30] a)M. M. Teeter, M. Froimowitz, B. Stec, C. J. DuRand, *J. Med. Chem.* **1994**, *37*, 2874; b)K. A. Neve, M. G. Cumbay, K. R. Thompson, R. Yang, D. C. Buck, V. J. Watts, C. J. DuRand, M. M. Teeter, *Mol. Pharm.* **2001**,

60, 373; c)H. Lan, C. J. DuRand, M. M. Teeter, K. A. Neve, *Mol. Pharm.* **2006**, *69*, 185; d)A. Mansour, F. Meng, J. H. Meador-Woodruff, L. P. Taylor, O. Civelli, H. Akil, *Eur. J. Pharm.- Mol. Pharm. Sec.* **1992**, *227*, 205.
[31] C. F. Matta, N. Castillo, R. J. Boyd, *J. Phys. Chem. B* **2005**, *110*, 563.
[32] M. J. Frisch, *et al*. *Gaussian 03, revision D.01*, Gaussian, Inc., Wallingford CT, **2004**.
[33] T. A. Keith, TK Gristmill Software, Overland Park KS, USA, **2012** (aim.tkgristmill.com).
[34] NBO Version 3.1, E. D. Glendening, A. E. Reed, J. E. Carpenter, and F. Weinhold.

SUPPORTING INFORMATION

Additional supporting information may be found in the online version of this article at the publisher's website.